EPJ Web of Conferences **259**, 12011 (2022) https://doi.org/10.1051/epjconf/202225912011
SQM 2021

First measurement of the B_c^+ meson nuclear modification factor in PbPb collisions with CMS

Guillaume Falmagne[1,*], on behalf of the CMS Collaboration

[1]Laboratoire Leprince-Ringuet, CNRS, École Polytechnique, Institut Polytechnique de Paris (91120 Palaiseau, France)

Abstract. The B_c^+ meson is observed in lead-lead and proton-proton collisions at a center-of-mass energy per nucleon pair of $\sqrt{s_{NN}}$ = 5.02 TeV, via the $B_c^+ \to (J/\psi \to \mu^+\mu^-)\mu^+\nu_\mu$ decay and using 2017 and 2018 data from the CMS detector. The resulting B_c^+ nuclear modification factor is measured in two bins of the trimuon transverse momentum and of the collision centrality. Less suppression is observed than for other quarkonia and most open heavy flavour mesons. This first observation of the B_c^+ meson in heavy ion collisions will shed light on the interplay of suppression and enhancement mechanisms in the production of heavy-flavor mesons in the quark-gluon plasma.

The extreme conditions of high-energy heavy-ion collisions allow quarks and gluons to move freely in a so-called quark-gluon plasma (QGP). The disappearance of quarkonia (as J/ψ or ϒ mesons) due to the screening of the heavy-quark potential at high temperature has been considered a signature of the QGP formation [1]. While the strong J/ψ suppression observed in heavy-ion collisions at lower energies [2, 3] seems consistent with screening effects, the smaller suppression reported at the Large Hadron Collider [4] points to the recombination of charm quarks in the QGP [5]. In the beauty sector, the suppression of ϒ(nS) states is sequential as expected from Debye screening [6], showing no evidence for recombination.

As the B_c^+ meson contains a charm and a beauty quark, measurements of its properties can bridge the gap between charmonia and bottomonia. The B_c^+ melting in the QGP is indeed expected to occur between the J/ψ and ϒ(1S) dissociation temperatures [7]. Heavy-quark recombination processes could also affect the B_c^+ state, with production rates typically scaling linearly with the charm multiplicity in the QGP (contrarily to a quadratic scaling for J/ψ mesons). It could lead to a large enhancement of the B_c^+ production in heavy ion collisions [7, 8] due to the rare B_c^+ production in pp collisions. This effect would mostly manifest at low transverse momentum (p_T) [7]. At large p_T, B_c^+ mesons are produced predominantly via heavy-quark fragmentation, hence probing the energy loss of a color triplet charge in the QGP (as observed for other B mesons [9, 10], J/ψ from B decays [11], and D mesons [12, 13]), whereas J/ψ mesons are mostly color octet states. Comparing the quenching of the B_c^+ meson with that of other heavy flavor mesons could therefore probe both the mass dependence of energy loss (from the dead-cone effect [14]) and its color charge dependence [15].

In this proceeding, the first observation of B_c^+ mesons in heavy ion collisions is reported. Charge-conjugate states are implicitly included in the following. We use data collected with the CMS detector in pp and PbPb collisions at $\sqrt{s_{NN}}$ = 5.02 TeV, corresponding to luminosities of 302 pb^{-1} and 1.61 nb^{-1}, respectively. The B_c^+ meson is partially reconstructed from the three muons in the $B_c^+ \to (J/\psi \to \mu^+\mu^-)\mu^+\nu_\mu$ decay mode.

The results are presented in two regions of the trimuon kinematic phase space: a low-$p_T^{\mu\mu\mu}$ bin, $6 < p_T^{\mu\mu\mu} < 11$ GeV with rapidity $1.3 < |y^{\mu\mu\mu}| < 2.3$, and a high-$p_T^{\mu\mu\mu}$ bin, $11 < p_T^{\mu\mu\mu} <$

*e-mail: guillaume.falmagne@cern.ch

35 GeV with $|y^{\mu\mu\mu}| < 2.3$. The PbPb results are shown for the 0–90% centrality range, and in the 0–20 and 20–90% ranges when integrated over the two studied kinematic regions.

A detailed description of the CMS detector can be found in Ref. [16]. Events of interest are selected using a two-tiered trigger system. The first level is composed of custom hardware processors. The high-level trigger runs a fast version of the event reconstruction software. This analysis uses events selected by double-muon triggers, with the same quality criteria for PbPb collisions as in Ref. [17].

Monte Carlo (MC) simulation is used for background studies and for estimating the acceptance and efficiency of the reconstruction and selection. B_c^+ mesons are generated with BCVEGPY2.2 [18] and decayed with EVTGEN1.3. The underlying event as well as prompt and nonprompt J/ψ background samples are generated with PYTHIA8.212, tune CP5. PbPb generated events are embedded into simulated collisions generated with HYDJET1.8. All samples are passed to GEANT4 to simulate the detector response.

The $B_c^+ \to (J/\psi \to \mu^+\mu^-)\,\mu^+\nu_\mu$ signal decay features three muons originating from the same displaced vertex, an opposite-sign muon pair consistent with the J/ψ mass, and a trimuon invariant mass $m^{\mu\mu\mu}$ between $m_{J/\psi} + m_\mu \simeq 3.2$ GeV and $m_{B_c^+} \simeq 6.3$ GeV. Three background sources can mimic this topology. Events with a fake J/ψ, where no muon pair comes from a J/ψ decay, are estimated by interpolating the data distributions between the lower and higher dimuon mass sidebands. B decays to a true J/ψ meson and a muon (usually a misidentified hadron) are estimated with simulation, constrained by previous measurements [11]. Its normalization is left unconstrained. The rotated J/ψ sample describes combinations of a true J/ψ with a muon (usually an uncorrelated misidentified hadron) from another decay. It is estimated by rotating the data J/ψ candidates around the collision vertex before associating them with third muon candidates. In PbPb collisions, the distributions from various rotation angles are identical and averaged. In pp collisions, significant J/ψ − μ correlations are considered by allowing the rotation angles to vary in the fit.

Offline selection criteria include the event-level and single-muon identification criteria defined in Refs. [17, 19], and loose single-muon kinematic acceptance criteria. One of the opposite-sign muon pairs must have an invariant mass in the J/ψ peak region, or in the sidebands. The sidebands and peak regions are taken to be of equal width. In case two opposite-sign dimuons are in those mass regions, two corresponding trimuon candidates are kept, weighted by the probability of being a true J/ψ. Requirements are also set on five variables dealing with the quality and the displacement of the trimuon vertex, the impact of the unreconstructed neutrino on the decay topology, and the collimation of the three muons.

A Boosted Decision Tree (BDT) is then trained on the selected simulated signal and above-mentioned backgrounds, combining the discriminating power of the selection variables and of three more topological ones. For each analysis bin, three BDT intervals are set to contain fixed fractions of the expected signal. The trimuon mass templates of signal and of the three backgrounds are fitted to pp or PbPb data, simultaneously in the three BDT intervals, and in the two analysis bins ($p_T^{\mu\mu\mu}$ or centrality).

The results of the fits integrated over the two kinematic bins are shown in Figures 1 and 2. The normalizations of the fake J/ψ sample, and the PbPb rotated J/ψ sample, are data-derived. Data yields and the signal-free high-mass region help determine the other normalisations.

The fitted signal yields are corrected for the acceptance and efficiency of the reconstruction and selection, calculated with the signal MC in each analysis bin. The simulated single-muon efficiencies are corrected with a tag-and-probe method [11]. The acceptance and efficiency are evaluated iteratively by first fitting the $p_T^{\mu\mu\mu}$ spectrum measured using the original MC. This allows to correct the $p_T^{\mu\mu\mu}$ spectrum of the MC before a second run of the analysis. A last $p_T^{\mu\mu\mu}$ spectrum correction is then performed, notably improving the acceptance and efficiency estimation. The corrected yields are then divided by the (pp-equivalent) luminosities.

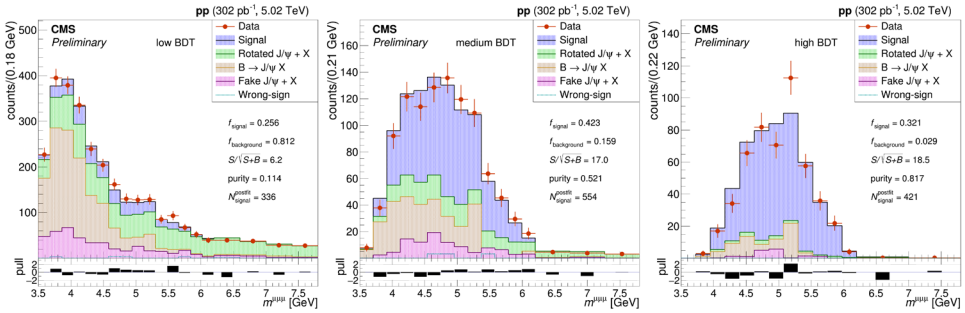

Figure 1. Template fit of the trimuon mass distributions in the three BDT bins, for the pp data sample integrated over the kinematic bins [20]. The pull between data and the fitted distributions is also shown.

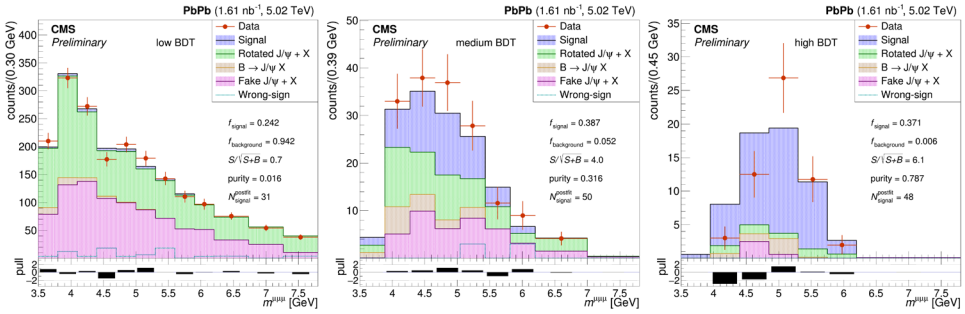

Figure 2. Template fit of the trimuon mass distributions in the three BDT bins, for the PbPb data sample integrated over the kinematic bins [20]. The pull between data and the fitted distributions is also shown.

Uncertainties arise from these sources: statistical, background shapes and normalizations, fit method, muon efficiency, B_c^+ kinematic properties, other B_c^+ decays, and overall normalization. The fit uncertainties, dominant in the PbPb $p_T^{\mu\mu\mu}$ bins, are both purely statistical and arising from background shapes and limited statistics; the latter are considered with nuisance parameters allowing variations of the background mass templates. The fit method is also varied, changing for example the $m^{\mu\mu\mu}$ or BDT bin limits or decorrelating the BDT variable from $m^{\mu\mu\mu}$. The uncertainties from the tag-and-probe, the luminosities, and the contamination from other B_c^+ decays as $B_c^+ \to J/\psi\tau^+\nu_\tau$, are sub-dominant. Since the B_c^+ kinematic spectra are not precisely known, acceptance and efficiency corrections are recalculated with toy p_T spectra obtained by fitting the measured p_T-differential yields varied within the above-mentioned uncertainties. The resulting uncertainty is the RMS of the varied acceptance and efficiency corrections or of the associated corrected yields; it dominates in the PbPb centrality bins.

The significance of the B_c^+ signal in PbPb collisions exceeds 5 standard deviations. Figure 3 shows the B_c^+ nuclear modification factor R_{PbPb}, as a function of $p_T^{\mu\mu\mu}$ (compared to open heavy flavour results from CMS) and of centrality. The latter is compared to unpublished predictions from the authors of Ref. [21] and based on similar transport model calculations on the B_c system, including correlated and uncorrelated recombination. The B_c^+ suppression is significantly lesser than for other heavy mesons [4, 6, 9, 11–13], except the B_s^0 meson [10], which may indicate that recombination is a significant B_c^+ production mechanism. The R_{PbPb} in the low-$p_T^{\mu\mu\mu}$ region stands above unity by 1 standard deviation, and above the high-$p_T^{\mu\mu\mu}$ region by 1.6 standard deviations, consistent with a softening of the p_T spectrum in the QGP. No centrality dependence is observed, contrarily to what the shown prediction suggests. The latter shows much more suppression than our result, possibly due to underestimating the recombination of B_c^+ excited states.

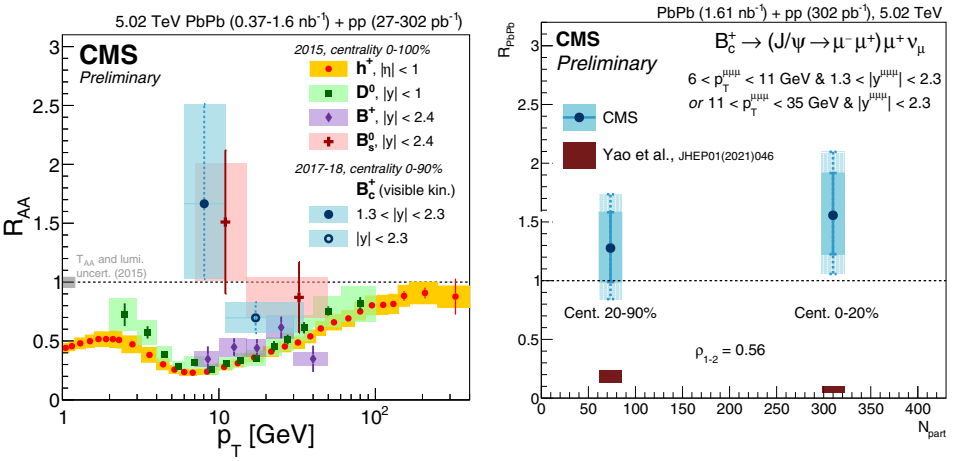

Figure 3. B_c^+ meson nuclear modification factor in $p_T^{\mu\mu\mu}$ bins corresponding to different rapidity ranges, from Ref. [20], compared to heavy-flavour measurements with CMS (*left*), and in centrality bins integrated over the studied kinematic range, compared to predictions from Yao et al. [21] (*right*). The solid and lighter rectangles, respectively, show the bin-to-bin-uncorrelated and total uncertainties.

In summary, the first measurement of the B_c^+ meson nuclear modification factor is presented, in PbPb collisions, in two bins of p_T or of centrality. This hybrid beauty-charm state can help discriminating the enhancement (possibly dominant in central events at low-p_T) and suppression (dominant at high-p_T) mechanisms in the dynamics of heavy quarks in the QGP.

References

[1] T. Matsui, H. Satz, Phys. Lett. B **178**, 416 (1986)
[2] M.C. Abreu et al. (NA50), Phys. Lett. B **477**, 28 (2000)
[3] A. Adare et al. (PHENIX), Phys. Rev. Lett. **98**, 232301 (2007), nucl-ex/0611020
[4] B.B. Abelev et al. (ALICE), Phys. Lett. B **734**, 314 (2014), 1311.0214
[5] P. Braun-Munzinger, J. Stachel, Phys. Lett. B **490**, 196 (2000), nucl-th/0007059
[6] S. Chatrchyan et al. (CMS), Phys. Rev. Lett. **109**, 222301 (2012), [Erratum: Phys.Rev.Lett. 120 (2018)199903], 1208.2826
[7] Y. Liu, C. Greiner, A. Kostyuk, Phys. Rev. C **87**, 014910 (2013), 1207.2366
[8] M. Schroedter, R.L. Thews, J. Rafelski, PRC **62**, 024905 (2000), hep-ph/0004041
[9] A.M. Sirunyan et al. (CMS), Phys. Rev. Lett. **119**, 152301 (2017), 1705.04727
[10] A.M. Sirunyan et al. (CMS), Phys. Lett. B **796**, 168 (2019), 1810.03022
[11] A.M. Sirunyan et al. (CMS), Eur. Phys. J. C **78**, 509 (2018), 1712.08959
[12] A.M. Sirunyan et al. (CMS), Phys. Lett. B **782**, 474 (2018), 1708.04962
[13] S. Acharya et al. (ALICE), JHEP **10**, 174 (2018), 1804.09083
[14] Y.L. Dokshitzer, D.E. Kharzeev, Phys. Lett. B **519**, 199 (2001), hep-ph/0106202
[15] F. Arleo, Phys. Rev. Lett. **119**, 062302 (2017), 1703.10852
[16] S. Chatrchyan et al. (CMS), JINST **3**, S08004 (2008)
[17] A.M. Sirunyan et al. (CMS), Phys. Lett. B **819**, 136385 (2021), 2006.07707
[18] C.H. Chang, et al., Comput. Phys. Commun. **174**, 241 (2006), hep-ph/0504017
[19] A. Tumasyan et al. (CMS) (2021), 2106.13235
[20] A.M. Sirunyan et al. (CMS), CMS-PAS-HIN-20-004 (2021)
[21] X. Yao, W. Ke, Y. Xu, S.A. Bass, B. Müller, JHEP **21**, 046 (2020), 2004.06746